

RSC Advances

Accepted Manuscript



This article can be cited before page numbers have been issued, to do this please use: W. Zhang, X. Lu, Z. Xin and C. Zhou, *RSC Adv.*, 2016, DOI: 10.1039/C6RA22524A.



This is an Accepted Manuscript, which has been through the Royal Society of Chemistry peer review process and has been accepted for publication.

Accepted Manuscripts are published online shortly after acceptance, before technical editing, formatting and proof reading. Using this free service, authors can make their results available to the community, in citable form, before we publish the edited article. We will replace this Accepted Manuscript with the edited and formatted Advance Article as soon as it is available.

You can find more information about Accepted Manuscripts in the [author guidelines](#).

Please note that technical editing may introduce minor changes to the text and/or graphics, which may alter content. The journal's standard [Terms & Conditions](#) and the ethical guidelines, outlined in our [author and reviewer resource centre](#), still apply. In no event shall the Royal Society of Chemistry be held responsible for any errors or omissions in this Accepted Manuscript or any consequences arising from the use of any information it contains.

Development of Superhydrophobic Polybenzoxazine Surface with Self-cleaning and Reversible Water Adhesion Properties

Wenfei Zhang, Xin Lu, Zhong Xin† and Changlu Zhou

Received 00th January 20xx,
Accepted 00th January 20xx

DOI: 10.1039/x0xx00000x

www.rsc.org/

A superhydrophobic polybenzoxazine surface has been developed by utilizing pendent aliphatic chain-substituted benzoxazine and TiO₂. Surface wettabilities, static and dynamic wettability, have been characterized by contact angle measurement. As a result, the prepared superhydrophobic polybenzoxazine/TiO₂ film exhibits static water contact angle of ~163±3° with low water sliding angle of ~1°, leading to self-cleaning property. This superhydrophobic polybenzoxazine/TiO₂ surface also has excellent resistance to solvents and corrosive liquids. Interestingly, this low-adhesive superhydrophobic surface switches to high-adhesive surface when exposed to UV light and transfers to the initial low adhesion when heated. The mechanism of the smart switch has been studied by using FT-IR, XPS and AFM. TiO₂ is responsible for the reversible water adhesion as it can absorb and desorb water molecular after UV irradiation and heat treatment. More importantly, along with the pendent aliphatic chains of polybenzoxazine, the surface maintains stable superhydrophobicity during the reversible switch.

Introduction

Bio-inspired superhydrophobic surfaces which has a static water contact angle (WCA) larger than 150° gain much research interest in self-cleaning surfaces,¹⁻⁴ micro droplet manipulation,⁵⁻⁹ anticorrosion coating and oil/water separation.¹⁰⁻¹² The performance of these applications based on superhydrophobic surfaces is largely determined by the mobility of water droplet on the surface.¹³ Based on different mobility of water droplet, superhydrophobic surface is generally divided into two types: low-adhesive and high-adhesive superhydrophobic surfaces.¹⁴ For specific applications, it is the adhesive property that ultimately determines the dynamic behavior of the liquid on the surface and appropriate adhesion is required.^{15, 16}

Recently, much attention has been paid to tunable water adhesion on superhydrophobic surfaces which means the

adhesion property is switchable between low and high on a superhydrophobic surface. This smart switch is expected to be more potential in various practical applications such as no loss micro droplet manipulation in fluidic devices, microfluidic chips and biochemical separation.¹⁷⁻²¹ Many studies have revealed that tunable water adhesion on superhydrophobic surfaces is mostly attributed to rational control of surface chemical compositions and surface microstructures. On one hand, Cheng et al have reported controllable water adhesion on Cu surface by adjusting the concentration of HS(CH₂)₁₁OH and HS(CH₂)₉CH₃ through self-assembling, which are used as modification agents.²² Similarly, tunable water adhesion on superhydrophobic surfaces with a large range of different WSAs from ~2° to ~90° have been fabricated by varying the composition of hydrophobic and hydrophilic ZnO nanoparticles.²³ These two groups develop tunable adhesive superhydrophobic surfaces by adjusting the surface chemical compositions. On the other hand, Yu et al have reported that high-adhesive superhydrophobic surfaces with honeycomb patterned microstructures on the surface can transfer to low-adhesive surfaces with pincushion-like microstructures by removing the top layer of the honeycomb and fluorinating the surface.²⁴ It can be found that most studies report tunable or controllable rather than reversible rolling-pinning switch of water adhesion by tailoring the surface chemical compositions or designing the surface microstructure on superhydrophobic surfaces so as to change the dynamic WCA (or WSA), which is the primary factor to control droplet move on surfaces.

To explore and develop reversible water adhesion on superhydrophobic surfaces, Liu and his co-workers have utilized pH-/thermal responsive polymer brushes to graft on a fluoroctyltrichlorosilane-modified rough surface and also

Shanghai Key Laboratory of Multiphase Structural Materials Chemical Engineering, State Key Laboratory of Chemical Engineering, School of Chemical Engineering, East China University of Science and Technology, 130 Meilong Road, Xuhui District, Shanghai 200237, People's Republic of China.

† Corresponding author: Tel. +86-21-64240862; Fax +86-21-64251772; E-mail xzh@ecust.edu.cn

Electronic Supplementary Information (ESI) available: Scheme S1. Synthetic procedures of P-da and P-am monomers and polymers. Figure S1. FT-IR spectra of P-da and P-am monomers and polymers. Figure S2. EDS spectrum of PPdaT80 surface. Figure S3. ¹H and ¹³C NMR spectra of P-am in DMSO-*d*₆. Figure S4. TGA thermograms of PPda and PPdaT80. The monomer and composite were polymerized at 200 °C for 1h, respectively. Figure S5. SEM images of PPdaT80 film (a) before and after UV exposure for (b) 1 h, (c) 5 h and (d) 9 h at low and high magnifications. Figure S6. AFM images of PPdaT80 film (a) before and after UV exposure for (b) 1 h, (c) 5 h and (d) 9 h at low and high magnifications. Table S1. Static WCA and WSA of PPamT80 before and after 5-hour UV exposure or heat treatment at 100 °C for 30min. Video S1. Self-cleaning performance of PPdaT80 film.. See DOI: 10.1039/x0xx00000x

reported an azobenzene-substituted PDMS film on a pre-roughened alumina surface.^{25, 26} Although the authors have found that water adhesions on these surfaces are switchable by external stimuli such as pH, heat and light, they have failed to gain a robust superhydrophobic surface or a cost-efficient and straightforward fabrication process because the substrate has had to be roughened at first and fluorination must be applied at last. However, one of the most noteworthy point is that the incorporation of nanoparticles into a polymer system is favorable to form micro- and nanoscale structures which are vital for preparing a superhydrophobic surface.²⁷ This strategy saves sophisticated surface roughening processes such as etching, templating and nanoimprint lithography.²⁸⁻³⁰

Except for the micro- and nanoscale structure, low surface free energy material is another key factor on surface wettability superhydrophobicity. Polybenzoxazine is a new type of low surface free energy material, and it is promising for a stable superhydrophobic surface due to its low water absorption and good thermal stability.^{31, 32} In our previous study, a silane-functional polybenzoxazine/TiO₂ superhydrophobic film with superhydrophobicity has been prepared by simple spin coating.³³ The results have indicated that the incorporation of responsive nanoparticles into low surface free energy materials is available for stimuli-responsive superhydrophobic surfaces. However, the previous work has only demonstrated a photo-induced reversibly switchable wettability of silane-functionalized polybenzoxazine/TiO₂ film that its superhydrophobicity converts to superhydrophilicity under UV stimulation, leading to an instable superhydrophobicity.

To overcome the limitations mentioned above, we demonstrate a stable pendent aliphatic chain-substituted polybenzoxazine/TiO₂ superhydrophobic surface with self-cleaning property and reversible reversibly switchable water adhesion through spin coating. This simple approach to achieving the robust superhydrophobic surfaces with smart switch of water adhesion may provide a convenient and an inexpensive platform for extensive applications of polybenzoxazine- based materials.

Results and discussion

Surface Morphology and Superhydrophobicity

Prior to the composite surface preparation, the chemical structure of benzoxazine monomer (P-da) has been confirmed by ¹H NMR and ¹³C NMR. As shown in the ¹H NMR spectrum of Figure 1, two characteristic singlet resonances located at 4.80 ppm and 3.90 ppm are attributed to the O-CH₂-N and Ar-CH₂-N of the oxazine ring, respectively, proving oxazine ring formation. The rest of the resonances at 2.60 ppm, 1.23 ppm and 0.85 ppm are related to the protons in aliphatic chain. The ¹³C NMR spectrum is also coincidence with the chemical structure of P-da. The resonances at 51.0 and 82.5 ppm are related to Ar-CH₂-N and O-CH₂-N of the oxazine ring, identifying the characteristic signal of oxazine ring. Additionally, regarding to the FT-IR spectrum of P-da in Figure S1, there is one band at 1227 cm⁻¹ being assigned to asymmetric stretching vibration of C-O-C, and the band at 934 cm⁻¹ which

is related to oxazine ring. Both of the NMR and FT-IR results proves the chemical structure of P-da. DOI: 10.1039/C6RA22524A

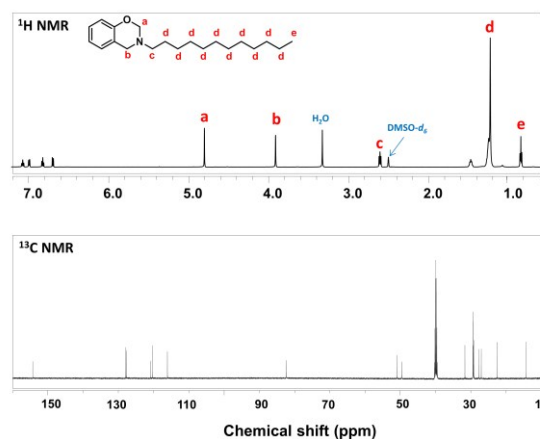
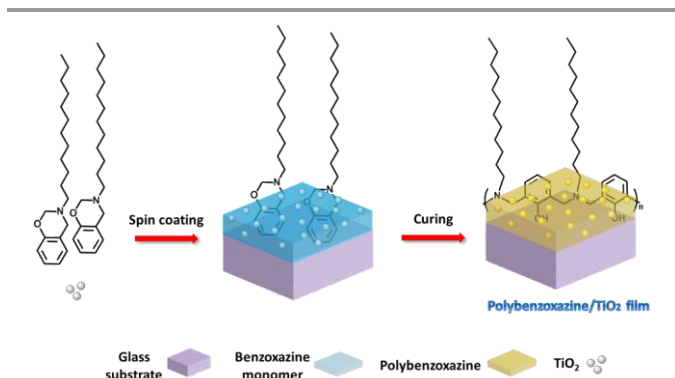


Figure 1. ¹H NMR and ¹³C NMR spectra of P-da in DMSO-*d*₆. The water signal comes from NMR solvent.

Thereafter, pendent aliphatic chain-substituted polybenzoxazine/TiO₂ (PPdaT) superhydrophobic surfaces were prepared by a simple spin coating and further thermal curing treatment as illustrated in Scheme 1. As shown in Figure S1, the absorption peak assigned to asymmetric stretching vibration of C-O-C at 1227 cm⁻¹ and bending vibration of C-H out plane at 934 cm⁻¹ disappears after heat treatment at 200 °C, which confirms the opening of oxazine ring and the occurrence of polymerization reaction. The formed polybenzoxazine can improve the surface hydrophobicity. Moreover, the introduction of TiO₂ nanoparticles is useful to increase surface roughness since proper roughness is a dominant factor on surface wettability.³⁴ Figure 2 shows the topographic structures of PPdaT surfaces with different content of TiO₂, and Figure 3 diagrams the variations in static WCA of PPdaT surfaces. The pure polybenzoxazine film without any TiO₂ has a flat surface (Figure 2a) with static WCA of ~104±1°. The PPdaT surfaces are obviously rough (Figure 2b-d), of which the static WCAs increase due to the enhancement of surface roughness. When the content of TiO₂ is 10 wt% or 30 wt%, the nanoparticles disperse sparsely and a rough surface is formed with a number of large grooves as shown in Figure 2b and 2c. Water droplets shall easily penetrate into the large groove, showing a static WCA smaller than 150° and a hydrophobic surface. Upon further increasing of TiO₂, a rough film such as PPdaT80 with relatively small and narrow grooves on the surface are achieved as shown in Figure 2d. Water could not totally penetrate into but mostly suspend on the top of the surface structures, demonstrating a large static WCA and a superhydrophobic surface. Accordingly, the difference in the surface morphology is reflected in physically macroscopic property wettability of PPdaT surface. The superhydrophobicity can be attributed to both the rough structures formed from TiO₂ and the surface modification of polybenzoxazine.



Scheme 1. Fabrication process of superhydrophobic PPdaT surfaces on glass substrate.

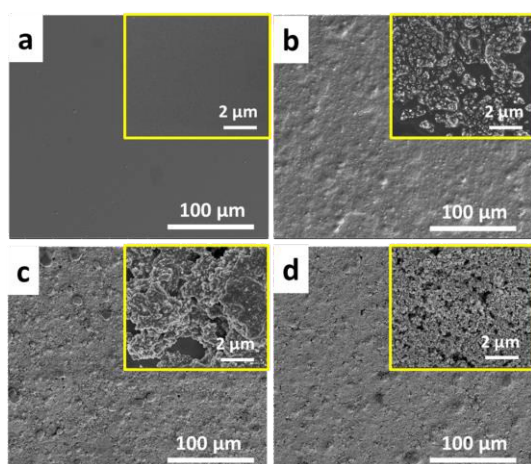


Figure 2. SEM images of (a) PPdaT0, (b) PPdaT10, (c) PPdaT30 and (d) PPdaT80 at low and high magnifications.

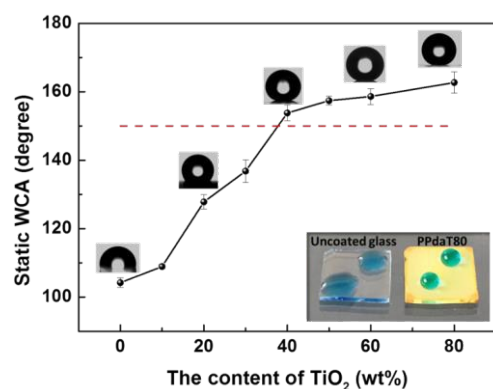


Figure 3. Variations in static WCAs of PPdaT surfaces with the relative mass percentage of different contents of TiO₂ to benzoxazine (P-da) monomer. The insets show the corresponding static WCA images of each sample and the photograph of water droplet on pristine glass substrate and PPdaT80 surface. Water was dyed with methylene blue.

To realize the wetting phenomenon of PPdaT surfaces, we also measured the advancing and receding contact angles by using an increment–decrement method. The water contact angle hysteresis (WCAH) is the difference of the advancing contact angle and the receding contact angle. The resulting static WCA, WCAH and WSA of each sample is listed in Table 1. WCAH values of hydrophobic pure polybenzoxazine film, PPdaT10 and PPdaT30 are all larger than 35° and there are no

specific WSA values can be measured out on these hydrophobic surfaces. Nevertheless, water droplets can roll off from these superhydrophobic surfaces with different WSAs. As a result, The higher the WCA is, the lower the WSA is. Water adhesion of the superhydrophobic PPdaT surfaces has been tuned effectively by adjusting the TiO₂ content, on which the WSA is controlled from ~22°, ~19°, ~4° to ~1° when the content of TiO₂ increases from 40 wt% to 80 wt%, respectively. Correspondingly, the WCAH of each sample decrease as well, demonstrating a rolling state.

Table 1. WCAH, WSA and static WCA of PPdaT surfaces.

Sample	WCAH (degree)	WSA (degree)	Static WCA (degree)
PPdaT0	~37	-	~104±1
PPdaT10	~46	-	~109±1
PPdaT20	~48	-	~128±2
PPdaT30	~39	-	~137±2
PPdaT40	~13	~22	~154±2
PPdaT50	~10	~19	~157±1
PPdaT60	~5	~4	~159±2
PPdaT80	~2	~1	~163±3

In addition, the presence of polybenzoxazine and TiO₂ on the surface is verified by energy dispersive spectrometer (EDS) characterization. As shown in Figure S2, the signals of carbon (C), oxygen (O) and titanium (Ti) atoms corresponding to PPdaT surface appear clearly in the EDS spectra. It can be concluded from the inserted mapping images that C and Ti atoms are distributed homogeneously on the PPdaT surface, indicating uniform distribution of polybenzoxazine and TiO₂ on the surface. A uniform distribution of the low surface free energy material polybenzoxazine and photo-responsive TiO₂ on the surface is important for the robust superhydrophobicity and good reversible water adhesion switch.

Self-cleaning and Robustness

Surface contamination can greatly affect the surface property and the performance of materials used in various field such as interior coating, oil/water separation and anti-corrosive coating, which calls for self-cleaning property.^{35–38} The as-prepared superhydrophobic PPdaT80 film in this work also enjoys good self-cleaning performance due to the large WCA of ~163±3° and small WSA of ~1°. As a proof of concept, the self-cleaning performance of PPdaT80 film has been carried out in a simple setup as shown in Figure 4. Water droplets can roll off together with the contaminations when the base is tilted for a small angle (<15°). Video S1 show that the water droplet adsorbs the contaminations and rolls off from the surface as it moves over the surface, showing a self-cleaning property of PPdaT80 surface. There is no self-cleaning observation on the pristine hydrophilic glass substrate, and the water droplets are pinned and stay on the surface when contacts on the surface. Moreover, the water stream that comes out from the syringe can bounce on the surface without leaving any water spot on the surface, revealing the very low-adhesive property of PPdaT80 surface. To justify the essential function of pendent aliphatic chains in PPdaT80 system on the self-cleaning property, a PPamT80 surface as a blank experiment has been prepared. It should be mentioned that

the benzoxazine monomer used for preparing PPamT80 has no pendent aliphatic chains. The molecular formula of P-am can be found in Figure S1. The ^1H NMR and ^{13}C NMR spectra of P-am have been illustrated in Figure S3, which confirms the chemical structure of this monomer without any hydrophobic pendent aliphatic chains. As listed in Table S1, the static WCA of PPamT80 is $\sim 155 \pm 1^\circ$, demonstrating the superhydrophobicity of PPamT80. However, since there is no pendent aliphatic chains in the benzoxazine molecular structure, water droplets adhere to the PPamT80 surface. In this case, there is no specific WSA value of PPamT80. Thus, the pendent aliphatic chains in polybenzoxazine exert an advantageous effect on the self-cleaning property.

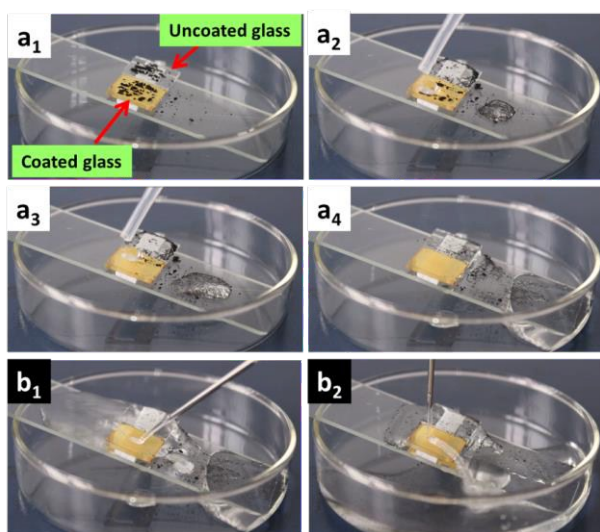


Figure 4. (a) Self-cleaning performance of PPdaT80 surface and (b) low adhesion property of continuous water stream on PPdaT80 surface.

In practical applications, the enhancement of durability and stability of a self-cleaning superhydrophobic surface in complex environments, such as long-term immerse in solvent, corrosive solution and hot water, is important. The as-prepared superhydrophobic PPdaT80 surface with low water adhesion has been conducted for durability and stability tests in detail. The as-prepared PPdaT80 surface exhibits excellent resistance to kinds of solvent even for 100 hours immersion at room temperature. As shown in Figure 5, the static WCAs of PPdaT80 film after being immersed in ethanol, toluene, tetrahydrofuran, acetone, dichloromethane and dimethyl sulfoxide are all above $\sim 160^\circ$, and the WSAs are all less than $\sim 3^\circ$. This solvent-resistant property of low-adhesive superhydrophobic PPdaT80 surface will be potential for separating oil/water mixture as the film can keep out the detrimental effects of these "oils" on the surface wettability and guarantee its low-adhesive superhydrophobicity.

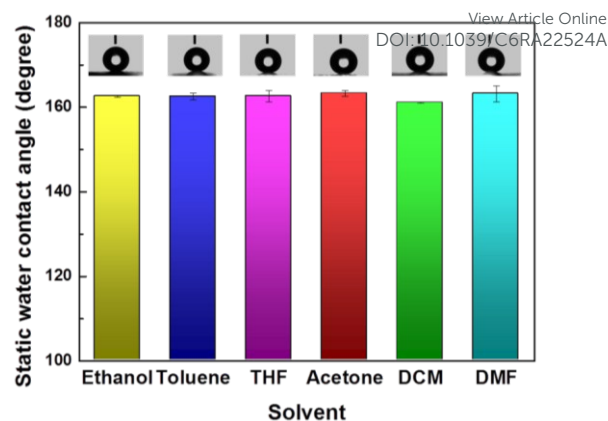


Figure 5. Static WCA of PPdaT80 surface after being immersed in ethanol, toluene, tetrahydrofuran, acetone, dichloromethane and dimethyl sulfoxide for 100 h at room temperature. The insets are corresponding WCA images of each sample. All the samples exhibit small WSA which is less than 3° .

Additionally, Table 2 lists the static WCA and WSA of PPdaT80 surface after being immersed in corrosive liquid and hot water at 80°C and heat treatment at 250°C . Since a general standard corrosive test utilizes the 3.5 wt% NaCl aqueous according to published works,¹⁰ herein, PPdaT80 has been totally immersed in 3.5 wt% NaCl aqueous solution for hours. It can be seen that the film has good resistance to a corrosive solution because the WCA is $\sim 159 \pm 3^\circ$ and the WSA is $\sim 20^\circ$ even though the surface is immersed in corrosive solution for 100 hours. Based on this property, PPdaT80 surface may pave a way for the preparation of anti-corrosive coatings with long-term use, which is significant in sustainable aspects. The superhydrophobicity of the film is also stable with WCA of $\sim 161 \pm 3^\circ$ and WSA of $\sim 8^\circ$ when it is placed in hot water at 80°C for 3 hours, which is more resistant to hot water than the reported fluorinated polybenzoxazine modified nanofibrous membrane under the same condition.⁴¹ It is noteworthy that the as-prepared superhydrophobic film maintains a large WCA of $\sim 163 \pm 2^\circ$ and a small WSA of $\sim 9^\circ$ even after heat treatment at 250°C owing to the good thermal stability of the polybenzoxazine resin. Moreover, the thermal stabilities of the polymerized P-da (PPda) and the representative composite PPdaT80 have been evaluated by using TGA as shown in Figure S4. P-da polymer obtains the char yield as 24 % at 800°C , while the composite 44% as show in Figure S4. Temperature of 5% weight loss and 10% weight loss for PPda and PPdaT80 are same and relatively high, which is 245°C and 286°C , respectively, demonstrating a good heat resistant property of the as-prepared polybenzoxazine composite. Overall, this superhydrophobic PPdaT80 film has self-cleaning property with good robustness. The film is durable and stable in solvents, corrosive solutions as well as hot water, which are advantageous in industrial applications.

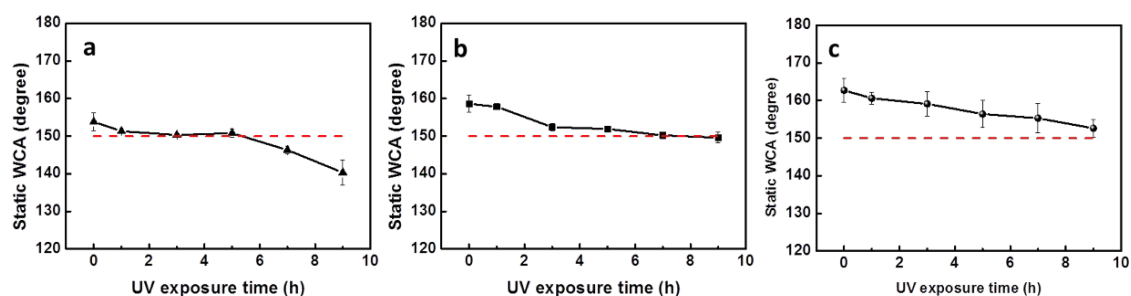
Table 2. Static WCA and WSA of PPdaT80 film after being immersed in corrosive liquid and hot water and heat treatment.

Condition	Static WCA (degree)	WSA (degree)
3.5 wt% NaCl, 100 h	~159±3	~20
Hot water at 80 °C, 3 h	~161±3	~8
250 °C, 1 h	~163±2	~9

Reversible Water Adhesion

The reversible rolling-pinning switch of water droplets on superhydrophobic PPdaT surfaces has been studied through UV exposure and heat treatment. As shown in Figure 6, the static WCA of each specimen goes down gradually with the

increasing shining time. After 9-hour UV irradiation, the static WCA of each sample has a decrease of 10°. Moreover, the PPdaT40 and PPdaT60 lost their superhydrophobicity with a static WCA of ~140±3° and ~149±1° after 9-hour irradiation due to the relatively lower static WCAs of initial surfaces. However, the PPdaT80 surface still maintains its superhydrophobicity with a static WCA change from ~163±3° to ~153±2°, showing a stable superhydrophobicity. In this work, we choose PPdaT80 which enjoys the stable superhydrophobicity under UV exposure to carry out a detailed investigation on the dynamic behaviour of water droplet on the surface.

**Figure 6.** Variations in static WCAs of (a) PPdaT40, (b) PPdaT60 and (c) PPdaT80 surface with various UV exposure times.

Interestingly, the variation in WSA of PPdaT80 under 9-hour irradiation changes dramatically. In Figure 7, the WCAH increases with the increasing of UV irradiation time. The WSA of PPdaT80 before UV exposure and after UV exposure for 1h is ~1° and ~17°, respectively, while the water droplets on the specimens after UV exposure for more than 5h are pinned on the surface when the base is tilted perpendicularly or is turned up-side-down, which is shown as the inserted images in Figure 7. Consequently, the 5-hour exposed superhydrophobic PPdaT80 surface with high water adhesion can be reversibly switched to its initial low water adhesion after heat treatment.

It can be summarized in Table 3 that the higher the treating temperature is, the lower the WSA is. The WSA of UV-exposed PPdaT80 after heat treatment at 100 °C for 30 min is ~2°, which is almost the same as the initial rolling state before UV stimulation. The water adhesion of PPdaT80 surface after the first UV exposure and the first heat treatment reveals a reversible rolling-pinning switch property of PPdaT80 surface as illustrated in Figure 8a. This reversibly switchable water adhesion can be repeated several times as shown in Figure 8b. The change of WCA in each cycle is about 10° and the surface after every treatment is still superhydrophobic.

ARTICLE

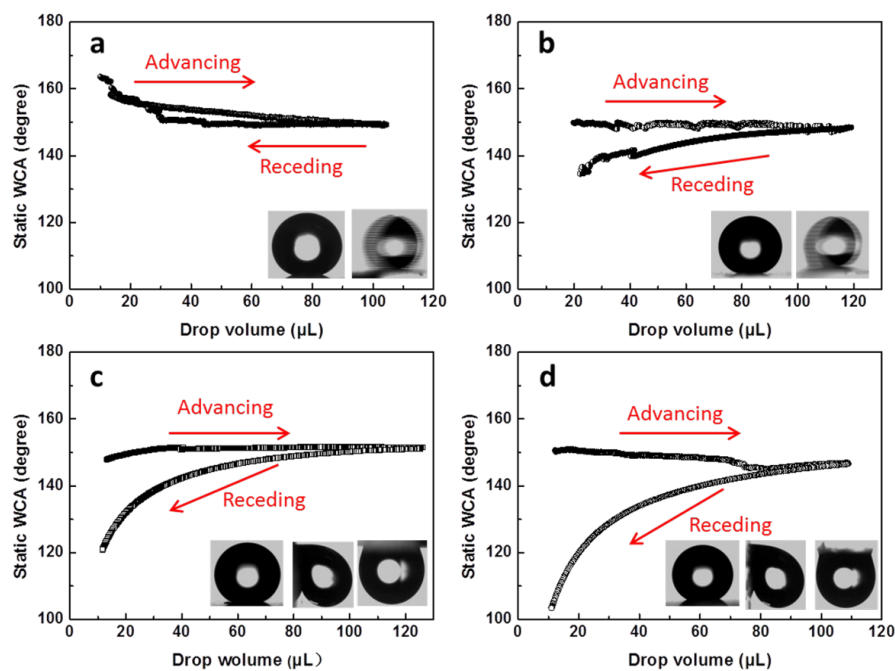
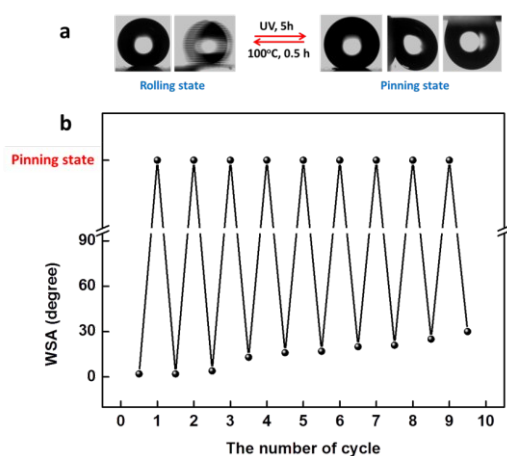


Figure 7. Advancing and receding WCAs of PPdaT80 (a) before UV exposure and after UV exposure for (b) 1 h, (c) 5 h and (d) 9 h by using an increment-decrement method. The insets show the corresponding WCA and WSA images of sample (a) and (b). The left, middle and right images in (c) and (d) are photographed when the base is tilted for 0° , 90° and 180° respectively.

ARTICLE

Table 3. Static WCA and WSA of UV-exposed PPdaT80 surfaces after heat treatment at various temperatures for 30 min.

Temperature (°C)	Static WCA (degree)	WSA (degree)
40	~160±4	~10
60	~161±2	~8
80	~162±2	~5
100	~161±1	~2

**Figure 8.** Reversible water adhesion on superhydrophobic PPdaT80 surface between UV exposure and heat treatment cycles.**Table 4.** Surface roughness and corresponding WCAH, WSA static WCA of PPdaT80 surfaces before and after UV exposure for 1 h, 5 h and 9 h.

Exposure time (h)	R_q (nm)	WCAH (degree)	WSA (degree)	Static WCA (degree)
0	~130±19	~2	~1	~163±3
1	~130±9	~15	~17	~161±2
5	~130±17	~31	-	~156±3
9	~129±15	~47	-	~153±2

The results of chemical composition analysis of PPdaT80 film reveal that the reversible water adhesion phenomenon is ascribed to the content of absorbed water molecules on the PPdaT80 surface after UV irradiation or heat treatment. In detail, Figure 9a shows that the intensity of the peak at 3415 cm^{-1} corresponding to the stretching vibration band of O-H in water molecular increases after UV irradiation, which indicates the existence of extra absorbed water molecules on the surface when PPdaT80 film is exposed under UV for 5 hour. It is the reason why the low adhesive superhydrophobic PPdaT80 film changes to high adhesive one. Water in the air is gradually absorbed onto the PPdaT80 film due to the typical photo-induced water adsorption feature of TiO_2 when the surface is placed under UV light.³⁹ Under this circumstance, water droplets impale on rough surfaces and are pinned on the surface with high adhesion. Moreover, the XPS spectra of Ti 2p peaks as well as the curve fitting peaks of Ti-OH (458.7 eV) and

Ti-O (459.0 eV) are shown in Figure 10. Obviously, the area fraction of the Ti-OH peaks increases and that of Ti-O decreases, indicating more water molecules absorbed on the surface after UV irradiation, thereby inducing the water droplets readily impaled on the surface and showing a high-adhesive PPdaT80 surface.

The mechanism of the reversible through sequential alternating of UV exposure and heat treatment has been proposed and discussed in detail. As mentioned in introduction section, through changing the chemical composition or morphology of a surface, the superhydrophobic wetting state can be controlled between low water adhesion and high water adhesion. Based on the surface roughness R_q values calculated from AFM characterization results and chemical composition analysis of PPdaT80 film by IR and XPS, it can be concluded that it is the chemical composition of PPdaT80 surface that dominates the reversibly adhesive property rather than the surface morphology or roughness. Table 4 lists the surface roughness R_q of PPdaT80 films before and after UV exposure for various times. It can be seen that the R_q of each sample keeps constant of around ~130 nm even though the WCAH and WSA vary greatly, which means that surface roughness is not a key factor on this reversible water adhesion phenomenon. Furthermore, as shown in Figure S5 and Figure S6, surface morphology of PPdaT80 before and after UV irradiation for various hours does not change too much, which further demonstrates that surface structure is not the main factor.

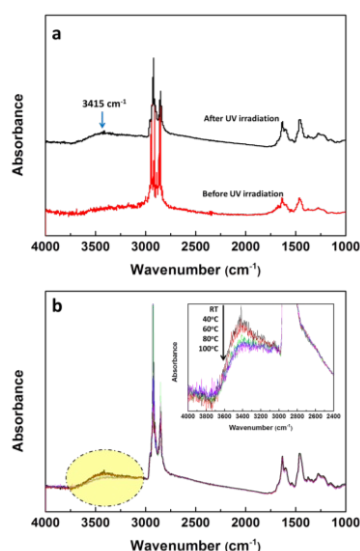


Figure 9. FT-IR spectra of superhydrophobic PPdaT80 (a) before and after UV irradiation. (b) FT-IR spectra of UV-exposed PPdaT80 after heat treatment at room temperature (RT), 40 °C, 60 °C, 80 °C and 100 °C for 30min respectively.

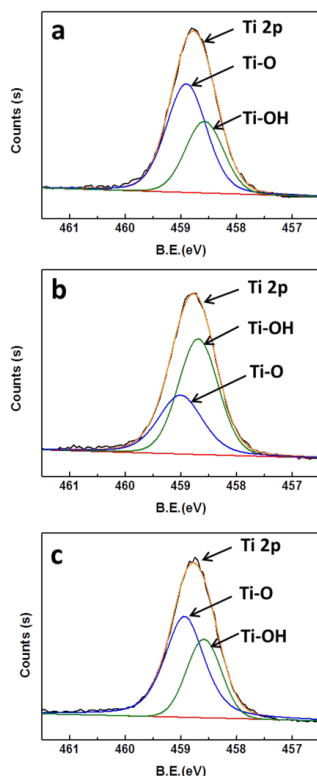


Figure 10. XPS (Ti 2p peaks) of (a) PPdaT80 film, (b) the film after the first UV light irradiation for 5 hours, and (c) the film after the first heat treatment at 100 °C for 30 minutes.

On the contrary, it can be observed that the intensity of peak at 3415 cm⁻¹ corresponding to the stretching vibration band of O-H in water in Figure 9b and the area fraction of the Ti-OH peaks in Figure 10 decrease after heat treatment. These results demonstrate the decreased content of absorbed water molecules on the surface when the exposed PPdaT80 film is heated at 100 °C for 30min. The less water absorbed on the surface or impaled in the micro-/nanostucture, the easier water droplets suspend on the top of the surface and the lower adhesion is.

Meanwhile, the pendent aliphatic chains in polybenzoxazine also exert an advantageous effect on the stable superhydrophobicity when UV light or heat triggers the switchable water adhesion. They prevent the water in air from totally wetting the surface and maintain the surface to be superhydrophobic. In order to justify the essential function of pendent aliphatic chains in PPdaT80 system on the surface superhydrophobicity, a PPamT80 surface as a blank experiment has been prepared, irradiated and then heated by using the same procedures. It should be mentioned that the benzoxazine monomer utilized for preparing PPamT80 has no pendent aliphatic chains. The molecular formula of P-am can be found in Figure S1. As listed in Table S1, before UV exposure, the PPamT80 film is superhydrophobic with a static WCA of ~155±1°, but it transfers to a hydrophobic surface and the static WCA decreases to ~101±3° after 5-hour UV exposure. The hydrophobic PPamT80 film cannot recover to its initial superhydrophobicity after the heat treatment at 100 °C for 30 min. Furthermore, no matter before or after UV irradiation, the PPamT80 shows high adhesion that water droplets are pinned on the surface. Therefore, the pendent aliphatic chains in polybenzoxazine keeps the surface superhydrophobic in a way of preventing the water droplet from totally wetting the film surface. The process of the reversible switch on superhydrophobic PPdaT80 can be illustrated in Figure 11. This simple approach to achieving smart photo-heat induced rolling-pinning switchable superhydrophobic surfaces may provide a straightforward and an inexpensive platform for extensive applications such as no loss micro droplet manipulation in fluidic devices, microfluidic chips and biochemical separation based on polybenzoxazine composite materials.

ARTICLE

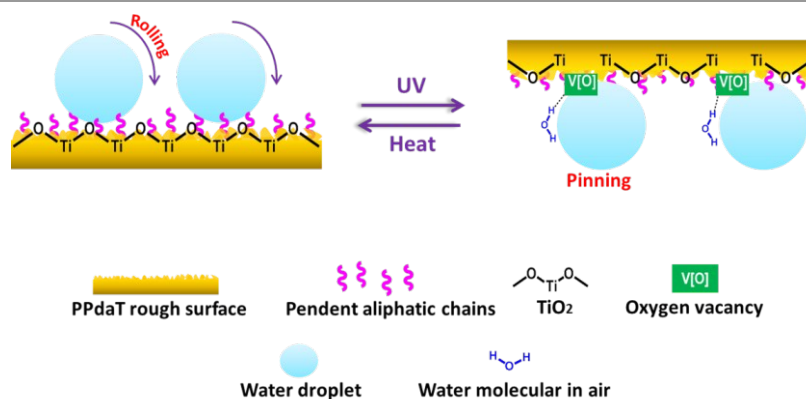


Figure 11. Proposed mechanism of reversible water adhesion on superhydrophobic PPdAT80 surface.

Experimental

Materials

Formaldehyde, phenol, 1,4-dioxane, ethyl acetate, sodium hydroxide and anhydrous sodium sulfate were purchased from Shanghai Lingfeng Chemical Corp. Ammonium hydroxide and dodecyl amine was obtained from Hubei Gravels Chemical New Material Corporation and Sinopharm Chemical Reagent Corporation, respectively. All chemicals were of analytical grade and used as received without further purification. Spherical TiO₂ nanoparticles (P25) with particles size of ~22 nm were kindly provided by the Evonik Degussa Specialty Chemicals Company. Glass slides (100×100×1 mm³) obtained from Hongda Medical Equipment Corporation was used as substrates.

Synthesis of 4-dodecyl -3,4-dihydro-2H-1,3-benzoxazine (P-da)

A pendent aliphatic chain-substituted benzoxazine was synthesized according to literature.⁴⁰ In detail, dodecylamine and phenol with molar ratio of 1:1 were mixed into a 250 mL three-neck flask. The system was stirred and, heated to 80 °C and kept for 10 min in an oil bath. Subsequently, in which 0.11 mol of paraformaldehyde was added into the system with vigorous stirring upon a further heating up to 110 °C. It continued to react for 2 h. The crude products were dissolved in ethyl acetate and washed with sodium hydroxide solution (2 M) for twice and then with water for three times. After being placed in anhydrous sodium sulfate overnight, the products were filtered and distilled out to obtain the benzoxazine monomer. The P-da obtained was yellowish and viscous. ¹H NMR (600 MHz, DMSO-*d*₆, ppm): δ =0.85 (t, 3H; -CH₂-(CH₂)₁₀-CH₃), 1.23 (m, 20H; -CH₂-(CH₂)₁₀-CH₃, overlapped), 2.60 (t, 2H; -CH₂-(CH₂)₁₀-CH₃), 3.91 (s, 2H; Ar-CH₂-N, oxazine ring), 4.80 (s,

2H; O-CH₂-N, oxazine ring), 6.68 (d, 1H), 6.81 (t, 1H), 6.98 (d, 1H), 7.06 (t, 1H). ¹³C-NMR (600 MHz, DMSO-*d*₆, ppm): δ =14.3, 22.5, 27.1, 27.8, 29.1, 29.3, 29.4, 29.5, 31.7, 49.7, 51.0, 82.5, 116.1, 120.4, 120.9, 127.7, 128.0, 154.3.

Synthesis of 3,4-dihydro-2H-1,3-benzoxazine (P-am)

P-am was studied as a blank experiment. Specifically, a solution of formaldehyde (0.11 mol of formaldehyde) in dioxane (50 mL) was added in a 250 mL four-neck flask. The system temperature was kept below 5 °C in an ice bath. Then, ammonium hydroxide (0.05 mol) dissolved in dioxane (20 ml) was mixed added into the system by dropping slowly and kept stirring for 10 min. Then, phenol (0.05 mol) in dioxane (20 ml) was added into the flask drop by drop. A reflux reaction continued for 6 h. The crude products were dissolved in ethyl acetate and washed with sodium hydroxide solution (2 M) for twice and then washed with water for three times respectively. After being placed in anhydrous sodium sulfate overnight, the products were filtered and distilled out to obtain the benzoxazine monomer P-am. These synthetic procedures were illustrated in Scheme S1. ¹H NMR (600 MHz, DMSO-*d*₆, ppm): δ =3.85 (s, 2H; N-CH₂-ArOH), 3.91 (s, 2H; Ar-CH₂-N, oxazine ring), 4.87 (s, 2H; O-CH₂-N, oxazine ring), 6.78-6.84 (m, 4H; overlapped), 6.98 (d, 1H), 7.10 (t, 2H; overlapped), 7.22 (d, 1H), 9.42 (s, 1H; OH). ¹³C-NMR (600 MHz, DMSO-*d*₆, ppm): δ =49.2, 50.2, 82.5, 115.6, 116.3, 119.3, 120.6, 120.7, 124.2, 127.8, 128.2, 128.4, 129.9, 154.2, 156.1.

Preparation of Polybenzoxazine/TiO₂ surfaces

The superhydrophobic pendent aliphatic chain-substituted polybenzoxazine surface was prepared based on Chinese patent.⁴² Glass substrates were pre-cleaned ultrasonically in deionized water, ethanol and acetone. Then, a certain amount of TiO₂ was added to benzoxazine monomer (0.10 g) solution (0.10 g) with a concentration of 10 wt% in THF. After holding

the benzoxazine/TiO₂ mixture in an ultrasound bath for 2 h to form a uniform dispersion, the mixture was spin-coated onto a glass substrate at 1500 rpm for 30 seconds. Finally, films were dried in vacuum oven at 60 °C for 1 h and polymerized at 200 °C for 1 h. The procedure is illustrated in Scheme 1. The polymerized nanocomposite samples were denoted as PPdaTx and PPamTy, where x and y is the relative mass percentage of TiO₂ to the weight of P-da and P-am monomers, respectively. e.g. PPdaT80, PPamT80.

Self-cleaning, Reversible Water Adhesion and Durability Test

To study the self-cleaning effect of the as-prepared surface, graphite powders scraped from pencil lead has been used as model contaminations. They were artificially fallen down onto the coated and uncoated glass. Then water droplet was directly dropped on the contaminated surface. The reversibly switchable water adhesion of PPdaT and PPamT films were conducted upon UV exposure and heat treatment. The UV light source was obtained from a 250 W Hg lamp. To measure the robustness of PPdaT, the hydrophobicity of as-prepared surfaces that totally and vertically immersed in ethanol, toluene, tetrahydrofuran, acetone, dichloromethane, dimethyl sulfoxide, HCl of 1 mol/L and NaCl of 3.5 wt% for 100 h at room temperature were examined by using contact angle measurement. Moreover, the samples were heated at 250 °C for 1 h and treated in hot water at 80 °C for 3h with magnetically stirring.

Characterization

Chemical structures of P-da, P-am monomers and polymers were characterized by IR spectroscopic measurements recorded with a Nicolet iS10 FTIR spectrometer. Solution of benzoxazine monomer in THF was directly dropped onto a KBr plate and formed a thin film after the solvent evaporation. To form poly(P-da) and poly(P-am) surface, the as-prepared monomer surface on KBr plate was further polymerized at 200 °C for 1 h. The results are listed in Figure S1. The temperature-dependent absorbance FTIR spectra were collected at room temperature utilizing a program heating cell and circulation air cooling system at 40 °C, 60 °C, 80 °C and 100 °C with a heating rate of 20 °C min⁻¹. Furthermore, ¹H NMR and ¹³C NMR were conducted on a Varian Oxford AS600 at a proton frequency of 600 MHz to confirm the chemical structure of benzoxazines. The average number of transients for ¹H and ¹³C NMR was 8 and 256, respectively.

A Data Physics OCA20 optical goniometer was used to measure static WCA at room temperature. The volume of deionized water droplet as 2 μL. The advancing and receding contact angles were measured by using an increment decrement method. The deionized water drop was inflated and deflated with an injection rate and suction rate of 1 μL s⁻¹. Then, water sliding angle (WSA) were measured with a tilting base. The deionized water droplet was 10 μL. The reported static contact angles represent the average of five measurements at different areas of surfaces.

Surface morphologies were observed with a Nova Nano SEM 50 field emission scanning electron microscope (FE-SEM). Chemical composition distribution of the film was

characterized by energy dispersive spectrometer (EDS) characterization in a mapping mode. Surface roughness profiles of surfaces were acquired using Veeco atomic force microscope (AFM) operated in a tapping mode. Each of the root-mean-square roughness (R_q) represents the average of three measurements over scan areas of 5 μm×5 μm. Chemical composition of the film was characterized by a ESCALAB 250Xi XPS and an Al K Alpha line excitation source with the reference of C 1s at 285.00 eV. Thermogravimetric analysis (TGA) was carried out on a TA instruments Q500 TGA with a heating rate of 10 °C/min under nitrogen at a flow rate of 60 mL/min.

Conclusions

In conclusion, a superhydrophobic polybenzoxazine composite surface is developed. The superhydrophobic polybenzoxazine surface with static WCA of ~163±3° and WSA of ~1° exhibits low water adhesion and excellent self-cleaning performance. In addition, its good resistance to solvents and corrosive liquids endows this polybenzoxazine-based superhydrophobic surface with great potential in oil/water separation and anti-corrosion field. It is interesting to mention that the as-prepared superhydrophobic polybenzoxazine surface also has a property of smart photo-heat induced reversible water adhesion. It will be advantageous to make a smart switch of micro devices such as in microfluidics and biochemical separation come true.

Acknowledgements

This work was financially supported by the Nanotech Foundation of Science and Technology Commission of Shanghai Municipality [0652nm001], Program of Shanghai Subject Chief Scientist [10XD1401500], National Natural Science Foundation of China [21506062], The Fundamental Research Funds for the Central Universities [22A201514015], China Postdoctoral Science Foundation [2015M571509], and Shanghai Key Laboratory of Multiphase Materials Chemical Engineering [MMCE2015004].

References

1. P. Wang, M. Chen, H. Han, X. Fan, Q. Liu and J. Wang, *J. Mater. Chem. A*, 2016, **4**, 7869-7874.
2. Y. Lu, S. Sathasivam, J. Song, C. R. Crick, C. J. Carmalt and I. P. Parkin, *Science*, 2015, **347**, 1132-1135.
3. Y. Liu, J. Chen, D. Guo, M. Cao and L. Jiang, *ACS Appl. Mat. Interfaces.*, 2015, **7**, 13645-13652.
4. S. Lathe, P. Sudhagar, C. Ravidhas, A. Christy, D. Kirubakaran, R. Venkatesh, A. Devadoss, C. Terashima, K. Nakata and A. Fujishima, *Cryst. Eng. Comm*, 2015, **17**, 2624-2628.
5. Y. Liu, X. Wang, B. Fei, H. Hu, C. Lai and J. H. Xin, *Adv. Funct. Mater.*, 2015, **25**, 5047-5056.
6. X. Yang, X. Liu, Y. Lu, J. Song, S. Huang, S. Zhou, Z. Jin and W. Xu, *J. Phys. Chem. C.*, 2016, **120**, 7233-7240.

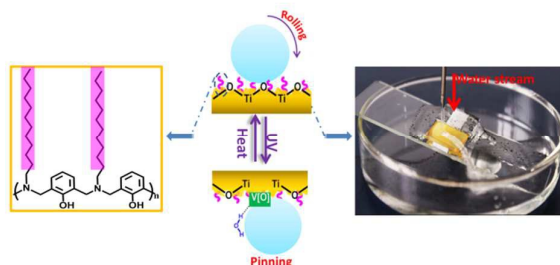
7. Y. P. Hou, S. L. Feng, L. M. Dai and Y. M. Zheng, *Chemistry of Materials*, 2016, **28**, 3625-3629.
8. A. Gao, Y. Zhao, Q. Yang, Y. Fu and L. Xue, *J. Mater. Chem. A*, 2016.
9. D. Zahner, J. Abagat, F. Svec, J. M. Frechet and P. A. Levkin, *Adv Mater*, 2011, **23**, 3030-3034.
10. C. Zhou, X. Lu, Z. Xin and J. Liu, *Corrosion Science*, 2013, **70**, 145-151.
11. W. Zhang, X. Lu, Z. Xin and C. Zhou, *Nanoscale*, 2015, **7**, 19476-19483.
12. Z. Xu, Y. Zhao, H. Wang, X. Wang and T. Lin, *Angew Chem Int Ed Engl*, 2015, **54**, 1-5.
13. D. Xia, L. M. Johnson and G. P. Lopez, *Adv Mater*, 2012, **24**, 1287-1302.
14. L. Wen, Y. Tian and L. Jiang, *Angew Chem Int Ed Engl*, 2015, **54**, 3387-3399.
15. P. Zhang, S. Wang, S. Wang and L. Jiang, *Small*, 2015, **11**, 1939-1946.
16. T. Liu and C. Kim, *Science*, 2014, **346**, 1096-1099.
17. D. Wu, S. Z. Wu, Q. D. Chen, Y. L. Zhang, J. Yao, X. Yao, L. G. Niu, J. N. Wang, L. Jiang and H. B. Sun, *Adv Mater*, 2011, **23**, 545-549.
18. H. Choi, S. Choo, J. Shin, K. Kim and H. Lee, *J. Phys. Chem. C*, 2013, **117**, 24354-24359.
19. L. Chen, W. Wang, B. Su, Y. Wen, C. Li, Y. Zhou, M. Li, X. Shi, H. Du, Y. Song and L. Jiang, *ACS Nano*, 2014, **8**, 744-751.
20. L. Tie, Z. Guo and W. Liu, *ACS Appl. Mat. Interfaces*, 2015, **7**, 10641-10649.
21. L. Hu, S. Gao, X. Ding, D. Wang, J. Jiang, J. Jin and L. Jiang, *ACS Nano*, 2015, **9**, 4832-4842.
22. Z. Cheng, R. Hou, Y. Du, H. Lai, K. Fu, N. Zhang and K. Sun, *ACS Appl. Mat. Interfaces*, 2013, **5**, 8753-8760.
23. J. Li, Z. Jing, F. Zha, Y. Yang, Q. Wang and Z. Lei, *ACS Appl. Mat. Interfaces*, 2014, **6**, 8868-8877.
24. X. Yu, Q. Zhong, H. Yang, L. Wan and Z. Xu, *The Journal of Physical Chemistry C*, 2015, **119**, 3667-3673.
25. X. Liu, Q. Ye, B. Yu, Y. Liang, W. Liu and F. Zhou, *Langmuir*, 2010, **26**, 12377-12382.
26. X. Liu, M. Cai, Y. Liang, F. Zhou and W. Liu, *Soft Matter*, 2011, **7**, 3331.
27. S. Yang, X. Jin, K. Liu and L. Jiang, *Particuology*, 2013, **11**, 361-370.
28. N. Liu, Y. Cao, X. Lin, Y. Chen, L. Feng and Y. Wei, *ACS Appl. Mat. Interfaces*, 2014, **6**, 12821-12826.
29. N. Gao and Y. Yan, *Nanoscale*, 2012, **4**, 2202-2218.
30. S. E. Lee, H. J. Kim, S. H. Lee and D. G. Choi, *Langmuir*, 2013, **29**, 8070-8075.
31. H. Ishida and D. Allen, *Journal of Polymer Science: Part B Polymer Physics*, 1996, **34**, 1019-1103.
32. C. Wang, Y. Su, S. Kuo, C. Huang, Y. Sheen and F. Chang, *Langmuir*, 2006, **22**, 8289-8292.
33. W. Zhang, X. Lu, Z. Xin, C. Zhou and J. Liu, *RSC Adv.*, 2015, **5**, 55513-55519.
34. F. Bottiglione and G. Carbone, *Langmuir*, 2013, **29**, 599-609.
35. S. Nishimoto, M. Ota, Y. Kameshima and M. Miyake, *Colloid Surf. A-Physicochem. Eng. Asp.*, 2015, **464**, 33-40.
36. P. Gao, Z. Liu, D. D. Sun and W. J. Ng, *J. Mater. Chem. A*, 2014, **2**, 14082.
37. C. Dai, N. Liu, Y. Cao, Y. Chen, F. Lu and L. Feng, *Soft Matter*, 2014, **10**, 8116-8121.
38. L. Zhang, Y. Zhong, D. Cha and P. Wang, *Sci. Rep.*, 2013, **3**, 2326.
39. J. Schneider, M. Matsuoka, M. Takeuchi, J. Zhang, Y. Horiuchi, M. Anpo and D. W. Bahnemann, *Chem. Rev.*, 2014, **114**, 9919-9986.
40. T. Agag, A. Akelah, A. Rehab and S. Mostafa, *Polymer International*, 2012, **61**, 124-128. DOI: 10.1039/C6RA22524A
41. X. Tang, Y. Si, J. Ge, B. Ding, L. Liu, G. Zheng, W. Luo and J. Yuc, *Nanoscale*, 2013, **5**, 11657-11664.
42. Z. Xin, W. Zhang, X. Lu, C. Zhou, *Chinese Patent Application*. 201610070931.8, 2016.

Table of Content

Development of Superhydrophobic Polybenzoxazine Surface with Self-cleaning and Reversible Water Adhesion Properties

Wenfei Zhang, Xin Lu, Zhong Xin* and Changlu Zhou

Shanghai Key Laboratory of Multiphase Materials Chemical Engineering, State Key Laboratory of Chemical Engineering, School of Chemical Engineering, East China University of Science and Technology, 130 Meilong Road, Xuhui District, Shanghai 200237, China



A superhydrophobic polybenzoxazine surface with self-cleaning performance is obtained, which is resistant to solvents and corrosive liquids.